

Original Research

Analysis of the Trade-offs/Synergies and Driving Forces of Ecosystem Services in the Yellow River Basin from 2000 to 2020

Chunyan Tian¹°, Keyu Han², Jianli Wei^{3*}, Wenhong Bai¹, Liuyang Yao¹

¹College of Economics and Management, North West Agriculture and Forestry University, Xianyang 712199, China

²College of Forestry, North West Agriculture and Forestry University, Xianyang 712199, China

³Xi'an Innovation College, Yan'an University, 710100, China

Received: 1 June 2024

Accepted: 24 February 2025

Abstract

The Yellow River Basin (YRB) has been central to China's strategy for achieving high-quality development by balancing ecological, economic, and social growth while ensuring environmental protection and restoration. Despite macro-level policy successes, detailed micro-level studies on the trade-offs, synergies, and driving forces of ecosystem services (ES) in this region remain limited. This study addresses this gap by examining the spatiotemporal dynamics, trade-offs, synergies, and driving forces of six key ES – soil conservation, food supply, habitat quality, water conservation, climate regulation, and wind and sand control – in the YRB from 2000 to 2020. Utilizing ecological models like InVEST and diverse data sources, including MODIS satellite imagery and climate databases, we quantified these ES and used Spearman's correlation coefficients along with spatial-temporal regression models to assess trade-offs and synergies. The Random Forest model and multiple linear regression were employed to identify ES drivers in both temporal and spatial dimensions. Results indicate significant spatial heterogeneity in ES within the YRB over the past two decades, with a general upward trend in service provision. The range of high and medium-value areas in each ecosystem gradually expanded while the range of low-value areas gradually shrank. Temporally, ES exhibited fluctuating but generally increasing trends. Among them, grain yield, soil conservation, and water conservation increased by 70.3%, 74.1%, and 17.7% on average. The synergistic effect between water resources protection and climate regulation is the strongest, with an average correlation coefficient of 0.39 in the past 20 years, while the trade-off between windbreaks and climate regulation caused by land use change is particularly prominent, with an average correlation coefficient of -0.3712. The analysis identified natural factors (NDVI, AET) and human activities (population density) as primary ES drivers. NDVI has an important impact on ecosystem services, and the contribution rate of NDVI to HA and HM is more than 40%. POP is dominant in HA and SR, especially in FP, with a driving degree greater than 40%. This research provides vital insights into YRB ES dynamics,

*e-mail: ydxxxy@163.com

°ORCID iD: 0009-0000-8680-949X

offering a scientific foundation for policies aimed at ecological sustainability and high-quality regional development.

Keywords: ecosystem services, trade-offs/synergies, Yellow River Basin

Introduction

In the past few years, the Chinese government has put forward an important strategy to promote the realization of high-quality development in the Yellow River Basin (YRB), to foster the synergistic development of the ecology, economy, and society of the Basin, and to ensure that the ecological environment of the Basin is effectively preserved and restored. Simultaneously, the excessive exploitation and utilization of natural resources are reduced through the promotion of green development, circular economy, and other models to provide a strong guarantee for the ecosystem services of the YRB. However, although high-quality development policies have played a positive role in the ecological protection of the YRB at the macro level, there is still a lack of comprehensive research on the trade-offs and synergies of ecosystem services in the YRB at a micro level, as well as an analysis of the driving forces behind these dynamics. An in-depth study on the long time series, multi-scale temporal and spatial change characteristics of ecosystem services, and driving force analysis in the YRB is of crucial significance for a deep understanding of the high-quality development policy in the YRB, as well as for the promotion of ecological protection in the YRB.

The term “ecosystem services” was first coined by Ehrlich et al. to refer to the range of tangible and intangible benefits that ecosystems provide to humans, including water conservation, soil conservation, climate regulation, etc., and which are essential for maintaining human well-being and regional ecological balance [1-4]. In the 1990s, Chinese scholars such as Xie Gaodi made localized modifications to the ecosystem service assessment method based on Costanza et al.’s study [5]. Through the establishment of the Equivalent Factor Method (EFM) ecosystem service valuation system, the method has become the mainstream method for scholars to evaluate the value of ecosystem services in the ensuing nearly 20 years. For example, Guo Hui et al. [6] analyzed the ecological carrying capacity of the ecological conservation and development zone in Mentougou District, Beijing, using the equilibrium factor and yield factor measurements of ecosystem service value. Linlin Zhang [7] and others proposed a regional correction factor to accurately assess the value of ecosystem services in the Sanjiang Plain of China based on the perspective of ecosystem service value and provide policy recommendations for ecological environment management, production efficiency, and ecological compensation. However, the method is mainly based on static estimation of statistical or survey data, which makes it difficult to finely quantify the spatial and

temporal characteristics of regional ecosystem services and the microscopic patterns of changes [8, 9]. Another group of scholars integrated remote sensing data and ecological parameter data to quantify regional ecosystem services with the help of ecological models such as Invest. For example, Xiaolan Yao et al. [10] applied the InVEST model and scenario analysis to explore the spatial and temporal patterns and impact analysis of rainforest ecosystem services on Hainan Island in southern China, and Yuxin Hua et al. [11] used the combined GeoSOS–FLUS–InVEST model to simulate the trends and spatial distributions of five essential ecosystem services under the three scenarios of the Natural Development Scenario, Policy Optimization Scenario, and Sustainable Development Scenario and explored the trade-offs and impacts among them. The trends and spatial distribution of the five essential ecosystem services under the natural development scenario, policy optimization scenario, and sustainable development scenario were simulated using the GeoSOS–FLUS–InVEST combined model, and the trade-offs and synergistic relationships among them were explored. However, most current studies are only analyzed for single indicators and lack an assessment of multiple ecosystem services [12-16]. In addition, the literature review shows a lack of integrated multi-scale and multi-indicator analyses of the Yellow River at long time series scales.

On the other hand, scholars have conducted a great deal of research on analyzing ecosystem service drivers. The mainstream methods are traditional mathematical and statistical analyses, such as correlation analysis and regression analysis. For example, Xiong Kangning et al. [17] used correlation and principal component analysis to explore the direct or indirect influence of various drivers on forest ecosystem service provisioning capacity in karst desertification ecosystems. Fang Guangji et al. [18] used correlation and regression analyses to explore the spatial and temporal dynamics of ecosystem service values in the Beijing-Tianjin-Hebei region of China and their trade-offs between urban and rural landscapes and concluded that improving ecosystem service trade-offs in urban and rural landscapes can promote urban-rural integration and provide policy insights for landscape governance. It also concludes that the urbanization rate is significantly negatively correlated with ecosystem services in the main urban area of Chongqing. However, the regression method needs to satisfy classical regression assumptions. It is prone to endogeneity problems where independent and dependent variables are causal to each other and are relatively weak in considering multi-factor interactions [19]. With the rapid development of geostatistical modeling, methods such as geo-weighted regression and geo-probe have been widely used

in regional ecosystem service driver analysis studies. For example, Dong Wei et al. [20] combined geodetector and geographically weighted regression to analyze the significant spatio-temporal heterogeneity of ecosystem services in the agro-pastoral zone and the analysis of the driving factors. Based on geodetector, Linghua Liu et al. [21] analyzed the driving factors for the changes in the value of ecosystem services in the Danjiangkou Reservoir Area from 2000 to 2018 and explored the land-use and land-cover changes [22-25]. This approach only supports the identification of spatial impacts on ecosystem services and cannot quantify the drivers of ecosystem services in the temporal dimension of the system. Therefore, this study used the random forest model and the absolute value standard deviation method of multiple linear regression to quantify the factors that influence the provision of ecosystem services in terms of space and time in the YRB [26-28].

To address the above deficiencies, this study quantified the ecosystem services of soil conservation, food supply, habitat quality, water conservation, climate regulation [29], and wind and sand control in the YRB from 2000 to 2020 based on ecological models such as Invest, quantified the multi-scale trade-offs/synergy analysis of ecosystem services using Spearman's correlation coefficients as well as image-by-image metrics of the temporal and spatial regression models, and finally used the random forest model and absolute value multiple linear regression model to investigate the drivers influencing ecosystem services in the YRB across both spatial and temporal dimensions. Specifically, this study aims to answer the following questions: 1) How do ecosystem services' long-time series spatial and temporal characteristics vary in the YRB watershed? 2) What are the trade-offs and synergistic characteristics of ecosystem services in the YRB at the grid and watershed scales? 3) What factors drive ecosystem services in the YRB in the spatial and temporal dimensions? This study has the following advantages over previous research: First, it employs a long time series and multi-scale spatiotemporal analysis to more comprehensively reveal the dynamic changes in the Yellow River Basin ecosystem services. Second, it conducts an integrated evaluation of multiple ecosystem service indicators, better understanding the synergies and trade-offs among different services. Third, it utilizes comprehensive models for quantification, enhancing the accuracy and reliability of the results. Fourth, it deeply explores the driving factors of ecosystem services, providing a basis for formulating more precise ecological protection policies.

Materials and Methods

Data Sources

Various types of data (Table 1) were utilized in this study. These included MODIS remote sensing

satellite imagery, HWSD soil database, elevation data, temperature data, precipitation data, Normalized Difference Vegetation Index (NDVI) data, and Terraclimate reanalysis data (see Table 1). Prior to analysis, all spatial data were transformed to the WGS 1984 coordinate system, and monthly data were combined to create annual data. The MODIS reflectance dataset underwent de-clouding using the CFMASK model, annual data were spliced and median synthesized, and the data were processed using Google Earth Engine.

Methods

This study uses ecological models such as Invest to quantify the ecosystem services in the Yellow River Basin from 2000 to 2020. At the same time, the Spearman correlation coefficient and graph-by-graph regression model were applied to quantitatively evaluate the multi-scale trade-offs and synergies of ecosystem services. Additionally, Theil-Sen median trend analysis and coefficient of variation analysis were used to explore the spatiotemporal evolution characteristics of ecosystem service supply. Finally, the random forest model and absolute multiple linear regression model were employed to investigate the spatiotemporal driving forces of ecosystem services from both temporal and spatial dimensions.

Water Conservation

The main function of the water supply is to control water flow by delaying the rise in subsurface runoff, managing surface runoff, and regulating river runoff by capturing and holding rainwater through the forest canopy, underground plants, deadfall layer, and soil. This task not only fulfills the water requirements of ecosystem elements but also guarantees an ample downstream water supply, highlighting its importance in providing diverse ecological services. This investigation utilizes the Water Balance Equation (WBE) to calculate water content.

$$Q_{WC} = P_i - R_i - ET_i \quad (1)$$

where Q_{WC} is water retention (mm yr^{-1}); P_i is rainfall (mm yr^{-1}); R_i is runoff (mm yr^{-1}); and ET_i is evapotranspiration (mm yr^{-1}).

Soil Conservation

In the study of soil conservation, the main emphasis is on how forest and grassland ecosystems can reduce erosion from rainfall. This involves the slow absorption of rain energy by layers of forest cover and decaying plant matter, which improves soil erosion resistance and decreases overall soil loss. Soil conservation is essential for maintaining ecosystem services like soil creation, water storage, plant stability, and ecological

Tab. 1. Detailed description of data.

Data name	Spatial resolution	Time resolution	Source	Note
MODIS	500 m	2000-2020	NASA. ^a	Classify LUCC
Sunshine hours	/	2000-2020	CMSDSSN. ^b	Calculate carbon sequestration
Soil texture	/	/	WSD. ^c	Calculate carbon sequestration
soil organic	/	/	WSD. ^c	Calculate carbon sequestration
soil capacity	/	/	WSD. ^c	Calculate carbon sequestration
Base pond area	/	/	WRDS. ^d	Calculate water retention
AET	4638 m	Monthly	NCAR ^e	Driven analysis at temporal scale
DEF	4638 m	Monthly	NCAR ^e	Driven analysis at temporal scale
PET	4638 m	Monthly	NCAR ^e	Driven analysis at temporal scale
RO	4638 m	Monthly	NCAR ^e	Driven analysis at temporal scale
SOIL	4638 m	Monthly	NCAR ^e	Driven analysis at temporal scale
SRAD	4638 m	Monthly	NCAR ^e	Driven analysis at temporal scale
TEMP	4638 m	Monthly	NCAR ^e	Driven analysis at temporal scale
PRE	4638 m	Monthly	NCAR ^e	Driven analysis at temporal scale
IBI	1000 m	Annual	Paper	Driven analysis at temporal scale
POP	1000 m	Annual	Paper	Driven analysis at temporal scale
CM	1000 m	Monthly	Paper	Driven analysis at temporal scale

Note: a, Resource and Environmental Science and Data Center (<https://www.resdc.cn/>). b, China Meteorological Science Data Sharing Service Network (<http://data.cma.cn/>). c, World Soil Database (<https://iiasa.ac.at/models-and-data/harmonized-world-soil-database>). d, Water Resources Department (<http://swt.hunan.gov.cn/>). e, National Center for Atmospheric Research (<https://climatedataguide.ucar.edu/>). f, National Aeronautics and Space Administration (<https://www.nasa.gov/>).

security. The calculation principles for soil conservation discussed in our research can be summarized as follows:

Actual soil erosion:

$$A_{AE} = R \times K \times L \times S \times C \times P \quad (2)$$

Potential soil erosion:

$$A_{PE} = R \times K \times L \times S \quad (3)$$

Soil conservation:

$$A_{SE} = A_{PE} - A_{AE} \quad (4)$$

A_{AE} measures the rate of soil erosion per unit area in ($t \text{ hm}^{-2} \text{ yr}^{-1}$); A_{PE} indicates the potential for soil erosion per unit area, measured in ($t \text{ hm}^{-2} \text{ yr}^{-1}$); A_{SE} denotes the soil retention per unit area in ($t \text{ hm}^{-2} \text{ yr}^{-1}$). The factor R for rainfall erosivity is a measure of the average annual rainfall erosivity index over multiple years; the soil erodibility factor K signifies the degree of soil erodibility; K is the measure of soil loss per unit area resulting from erosion caused by a standardized amount of rainfall under a standard plot; The slope length factor (L) and the slope factor (S) are both dimensionless

variables that contribute to understanding terrain variability; L accounts for the influence of slope length on erosion, while S accounts for the influence of slope steepness. The factor for vegetation cover (C) and the factor for soil and water conservation measures (P) are also dimensionless and are used to delineate the impact of ground cover and conservation practices, respectively, on soil erosion rates.

Carbon Sequestration Services

Green plants play a crucial role in services related to carbon sequestration, as they absorb carbon dioxide (CO_2) through photosynthesis. During this process, they transform carbon dioxide into carbohydrates like glucose, storing it as organic carbon within their structures or in the soil. This function is significant for maintaining climate regulation, as it helps balance CO_2 levels in the atmosphere. Furthermore, it contributes to reducing the impact of the greenhouse effect and enhances the overall environmental quality. The study's evaluation criterion was based on the extent of carbon sequestration utilized. This metric was used to assess the effectiveness of ecosystems in performing the essential function of carbon sequestration.

$$NEP = NPP - R_h \quad (5)$$

$$R_h = 0.592 \times R_s^{0.714} \quad (6)$$

$$R_s = 1.55e^{0.031 \times T} \times \frac{P}{P + 0.68} \times \frac{0.58 \times BD \times H \times (1 - \delta / 100) / 10}{0.58 \times BD \times H \times (1 - \delta / 100) / 10 + 2.23} \quad (7)$$

NEP signifies carbon capture within ecosystems measured in grams of carbon per square meter per year ($\text{g C m}^{-2} \text{ yr}^{-1}$), while NPP stands for the ecosystems' net primary productivity, also quantified as ($\text{g C m}^{-2} \text{ yr}^{-1}$). R_s denotes carbon usage through soil respiration, measured similarly in ($\text{g C m}^{-2} \text{ yr}^{-1}$). On the other hand, T denotes the average annual air temperature, and P signifies the total yearly precipitation. BD is the bulk density, expressed as grams per cubic centimeter (g cm^{-3}). H represents the soil depth of 20 cm, and δ indicates the percentage of soil particles smaller than 2 mm.

Habitat Quality

HQ refers to the ability of ecosystems to provide conditions suitable for the persistence of individuals and populations, which is one of the important supporting services. High-quality habitats can provide more resources for population survival to better support different levels of biodiversity. We modeled HQ using the InVEST model, which calculates habitat quality by combining the stress intensity of different land use/land cover (LULC) types and their sensitivity to threat factors. HQ was calculated using the following formula:

$$Q_{xj} = H_j \times \left(1 - \frac{D_{xj}^z}{D_{xj}^z + k^z}\right) \quad (8)$$

where Q_{xj} is the HQ value of grid x ; H_j is the habitat suitability of LULC type j ; D_{xj} is the habitat degradation degree of grid x ; z is a scaling parameter; and k is the half-saturation constant, which was set at 0.05. Except for LULC data, the threat factor table and sensitivity table are required for the InVEST model. The coefficients of threat factors, habitat suitability values, and habitat types sensitivity to threat factors were referenced from the study in similar areas.

Food Production

FP, one of the crucial provisioning services for mankind's survival and development, refers to the food produced by terrestrial ecosystems. In alignment with previous studies, we quantified FP by combining NDVI data with agricultural statistics from statistical

yearbooks. The food yield data were derived from the Chinese Statistical Yearbook.

$$Y_i = A \times \frac{NDVI_i}{NDVI_{sum}} \quad (9)$$

where Y_i is the total yield of food in grid cell i , A is the total yield of food, $NDVI_i$ is the NDVI value of the i_{th} pixel, and $NDVI_{sum}$ is the total value of NDVI.

Climate Regulation

This study used the degree of local cooling by ecosystems to characterize the ecosystem's climate regulation. First, we calculated the mean annual land surface temperature based on the Google Earth Engine platform, then set the cooling intensity of water and bareland to 0. Next, we calculated the mean surface temperature of each ecosystem type for each year and then subtracted the mean surface temperature of bareland from the mean land surface temperature of all ecosystem types (except water and bareland).

$$CE = T_i - T_{Bareland} \quad (10)$$

where CE is the climate regulation function, T_i is the land surface temperature of the i_{th} pixel, and $T_{Bareland}$ is the average land surface temperature of the bareland.

Ecosystem Service Trade-offs and Synergies

In this study, the examination concentrated on analyzing the balance and harmonious connections among ecosystem services (ESs) through statistical techniques at both country and pixel scales. Spearman correlation coefficients were employed at a significance level of 0.05 to quantify the correlation between ESs. A negative correlation coefficient indicated a trade-off relationship between the ES pair, while a positive correlation coefficient indicated a synergistic relationship.

$$R_{mn} = \frac{\sum_{i=1}^x (m_i - \bar{m})(n_i - \bar{n})}{\sqrt{\sum_{i=1}^x (m_i - \bar{m})^2 \sum_{i=1}^x (n_i - \bar{n})^2}} \quad (11)$$

where the correlation coefficient between variables m and n is denoted as R_{mn} . The ESs for year i are represented as m_i and n_i . The variable x is used to denote the year, and in this particular paper, x is equal to 5.

Random Forest Importance Analysis

The popular learning algorithm, the random forest model, is commonly used in ecosystem services research

as it combines multiple decision trees. Random and putative sampling methods were utilized in this study to construct each decision tree. For the training set, 4/5 of the samples were used, and the remaining 1/5 were held for accuracy verification, referred to as Out-Of-Bag data (OOB). Calculating the OOB misclassification rate involves determining the ratio of misclassifications to the total number of samples, serving as a crucial measure to assess the significance of feature variables.

We employed the replacement method to calculate the OOB misclassification rate. Initially, we calculated the OOB misclassification rate under normal conditions. Then, we replaced the value of X_j and recalculated the OOB misclassification rate [30, 31]. The difference between the two rates represents the importance of the variable X_j in each tree, which can be calculated using the following formula.

$$VIM_j^{OOB} = \frac{1}{n} \sum_{i=1}^n (Error_j^i - Error_i) \quad (12)$$

where VIM_j^{OOB} is the importance of feature variable j , $Error_i$ is the misclassification rate before replacement, and $Error_j^i$ is the misclassification rate after replacement.

Conclusion of Methods

This study was conducted based on multiple ecological process models and several geostatistical models. The innovation lies in the combination of ecological and statistical methods and knowledge to quantify the trade-offs/synergies of ecosystem services in the Yellow River Basin over the past two decades, as well as their driving factors.

Results and Discussion

Spatial and Temporal Changes Characteristics of Ecosystem Services

Spatial Dimension

In this research, a comprehensive assessment of ecosystem services such as water retention (WR), habitat quality (HA), soil conservation (SR), food production (FP), wind and sand control (SL), and climate regulation (HM) was carried out in the YRB during 2000 and 2020 (Fig. 1). From the assessment results, these ecosystem services showed significant spatial heterogeneity within the YRB. In the past two decades, the ecosystem services in the YRB have been characterized by obvious spatial differentiation, with the range of high and medium-value zones gradually expanding and the range of low-value zones gradually shrinking in each ecosystem. Specifically, the FP high-value areas are point-like distributed in densely populated areas near the YRB, such as the Ningxia Plain and the Hetao Plain in the northwestern part

of the basin and the Fenwei Plain in the downstream part of the basin. They tend to expand and gradually advance from the southeast to the northwest. Low-value areas are faceted in sandy and desert areas, hilly and gully areas, the northern part of the high loess gully area, and other areas where the population is more dispersed, with less arable land and low food production per unit area [32]. WR and SR services decreased gradually from south to north, with an obvious stratified stepwise distribution. Water production services and soil conservation in the southern Ningxia and Shandong basins were significantly improved, thanks to the gentle topography and favorable climate, and the WR and SR levels were higher. The Qilian Mountains and the Jin-Shaan-Yu basin (i.e., the middle reaches of the Yellow River) showed a significant decrease in WR and SR levels due to ecological degradation caused by frequent soil erosion [33]. HA and HM show a hierarchical stepwise distribution decreasing from the southeast to the northwest, with high values mainly in the highland meadows and mountainous woodlands in the southwest of the basin, while low values are mainly located in the desert areas in the central part of the basin and in parts of the northwest [34]. SB is the characteristic ecosystem service level of the YRB, which refers to the inhibition and fixation of wind and sand by vegetation ecosystems [35]. The high-value areas of windbreaks and sand fixation per unit area are distributed in the western and northwestern regions of the Basin, including Gansu, southern Ningxia, southern Yulin in Shaanxi, Guanzhong Plain, southwestern Shanxi, and part of Henan, and low-value areas are located in the southern part of the Basin and the lower reaches of the Yellow River, including Inner Mongolia, north-central Shanxi, and Jinan Dongying in Shandong.

Time Dimension

From the time scale, the supply of food production, soil conservation, habitat quality, climate regulation, wind and sand control, and water conservation in the ecological functional areas of the YRB from 2000 to 2020 changed significantly over time, and the ecosystem services showed a general trend of growth (Fig. 2).

Specifically, grain output in the YRB showed a fluctuating trend of increasing-increasing-decreasing-increasing, with a total increase of 38.505 kg/cell and an average increase of 70.333%. Among them, the grain output was the highest in 2020 and the lowest in 2000. In terms of the spatial distribution of changes, the areas with the largest increases were located in the southeastern part of the watershed, such as Slip County in the northeastern part of Henan province, Yanjin County in the northern part of Henan province, and Qihe County in the western part of Shandong province, etc.; the changes in the habitat quality index were small, showing a fluctuating trend of increase-increase-decrease-increase, with an enhancement of 0.021, with an average increase of 7.609%. Spatially,

the regions with the largest increase in the habitat quality index were mainly distributed in Yulin City in northern Shaanxi Province, Tianshui City in southern Gansu Province, and Maowusu Sandy Area in Inner Mongolia. When it comes to the distribution of space, the trend of grain production and habitat quality showed

a similar distribution pattern, with the increase in areas mainly distributed in the eastern and southern parts of the basin; climate regulation showed a fluctuating trend of increase-increase-increase-decrease, with an average increase of 0.422%, and spatially, the areas with the largest increase were located in the northwestern

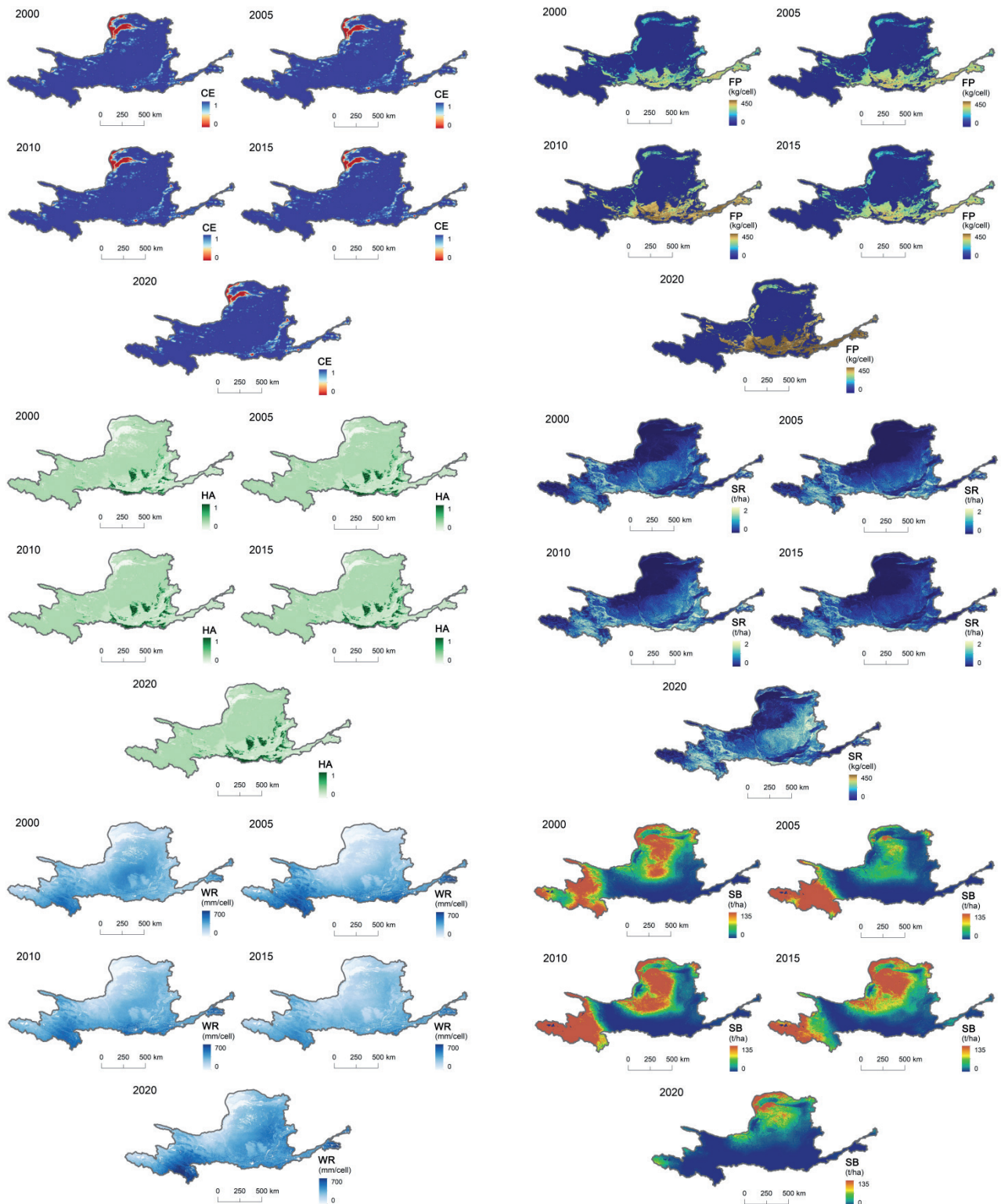


Fig. 1. Spatial and temporal distribution of climate regulation (CR), food production (FP), habitat quality (HQ), soil conservation (SC), sand break (SB), and water conservation (WC) in the Yellow River Basin, 2000-2020.

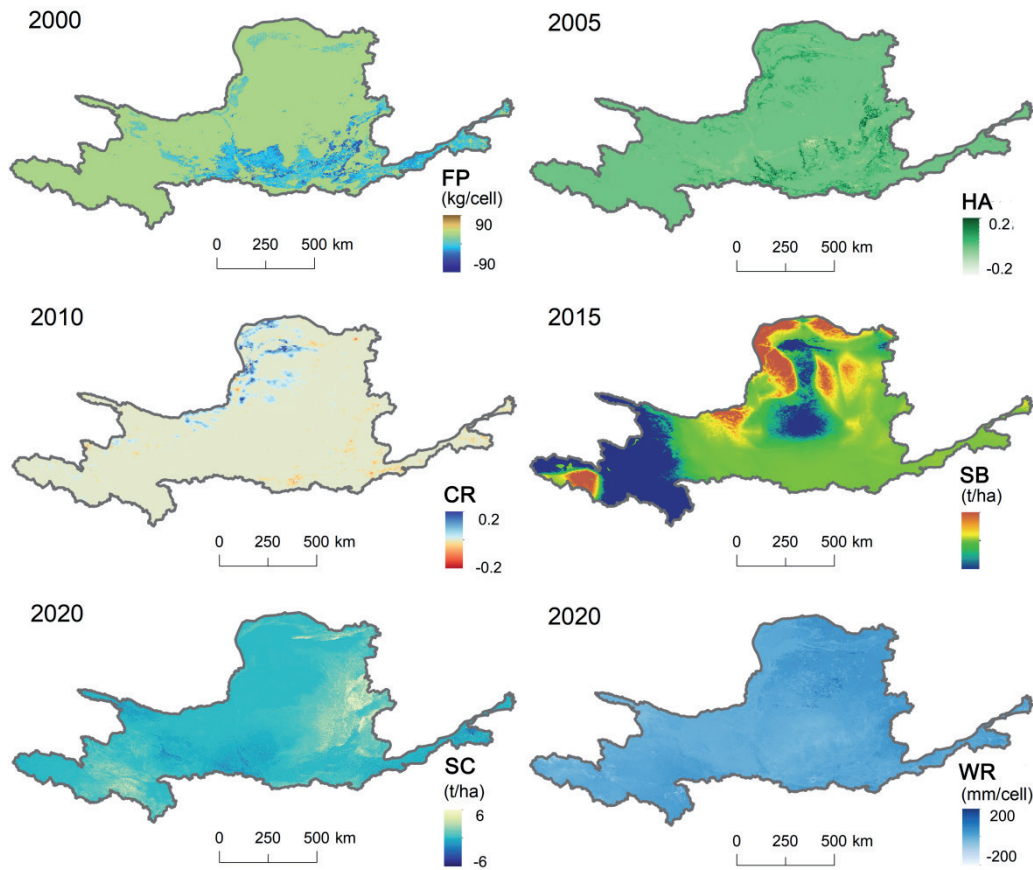


Fig. 2. Spatial and temporal trend of climate regulation (CR), food production (FP), habitat quality (HQ), soil conservation (SC), sand break (SB), and water conservation (WC) in the Yellow River Basin, 2000-2020.

Ningxia Plain, the Hetao Plain, and the area near the Mao Wusu Sandy Land; the amount of wind- and sand-fixing services was the highest in 2010, with the highest increase in the amount of wind and sand-fixing services. The amount of windbreak and sand fixation services was the highest in 2010. When it comes to the spatial distribution of changes, the regions with the largest increases were located in the Hetao Plain, Loess Plateau, and areas near the Mao Wusu Sandy Land, as well as in areas such as Maqin County in southern Qinghai; the soil conservation showed a fluctuating trend of decreasing-increasing-decreasing-increasing, with an average increase of 74.138%, and spatially, the areas with the largest increases were located in Maqin County, northern Shanxi Province, Xinzhou City, northern Taiyuan City, and other areas in the north. The fluctuating trend of increase-increase-decrease-increase in water conservation, with an average increase of 17.677%, and spatially, the areas with the largest increase are located in Maqin County in southern Qinghai Province, Jinan City in central and western Shandong Province, and Zhengzhou City in north-central Henan Province, etc. The other areas' changes are not significant, showing an alternating pattern of increase and decrease in distribution, with no centralized trend in distribution. There is no centralized distribution trend. In summary, ecosystem services in

the YRB differ significantly in spatial distribution and show an overall increasing trend in time.

Trade-off Synergies for Ecosystem Services

Spatial Scale

According to the pixel scale, this study measured and analyzed the trade-offs and synergies among the six ESs in the YRB using the Spearman system (Fig. 3), and a total of 15 trade-offs and synergies were obtained. Overall, significant synergies between various types of ecosystem service functions dominated in the last 20 years. Of these, 9 synergistic relationships and 6 trade-offs in 2000 and 2010, 11 synergistic relationships and 4 trade-offs in 2005, and 8 synergistic relationships and 7 trade-offs in 2015 and 2020. 14 out of 15 relationships passed the significance test ($p < 0.05$), and the difference was statistically significant. Of all the relationships, the strongest synergy was between water harvesting and climate regulation in 2000, 2010, 2015, and 2020. Water harvesting provides a stable water resource base for climate regulation, while climate regulation helps to maintain the long-term stability of water harvesting by reducing greenhouse gas levels. The strongest synergistic relationship in 2005 was water conservation-soil conservation, which helps the soil

retain moisture and maintains the stability of the soil structure through the conservation and management of surface and groundwater resources. In turn, a stable soil structure further promotes water conservation, creating a virtuous cycle [36]. The strongest trade-off in 2000, 2015, and 2020 is windbreak-climate regulation, with a negative correlation to the climate regulation function due to the conversion of forested and grassed land used for windbreak into cropland, built-up land, etc., which affects the vegetation cover on the surface and disrupts the structure of the soil and the hydrological cycle [37]. The strongest trade-off in 2005 and 2010 was food supply-habitat quality, where the excessive application of pesticides or fertilizers in agricultural practices aimed at boosting crop yields frequently results in detrimental consequences such as the decline of biodiversity and contamination of water sources [38].

The ES pairs related to wind and sand conservation in 2000, 2010, 2015, and 2020 all showed trade-offs, indicating that the rise in wind and sand conservation functions over the past 20 years has decreased the functionality of other ecosystem services. For example, to enhance the wind and sand control services, managers may adopt specific land use and management strategies, such as changing the vegetation structure and adjusting the planting density, reducing the vegetation cover on the ground surface, and decreasing soil retention and water-holding capacity [39].

Time Scales

The map in Fig. 4 illustrates the trade-offs and synergies of ecosystem services in the YRB from 2000 to 2020 at the pixel scale, where most ESs are in weak synergistic relationships at the pixel scale (temporal dimension). SOIL synergizes with HA, HM, WR, FP,

and SL. The study found that while land use/land cover change (LUCC) plays a significant role in determining the spatial distribution of ecosystem services (ES) in the YRB under a static dimension [40], the interactions between ES in a dynamic dimension are primarily influenced by physical processes such as energy exchange and material cycling among vegetation, hydrology, and meteorology [41]. This discrepancy results in weak synergistic relationships between most ES functions and LUCC (except FP), which contradicts the outcomes of trade-off/synergistic analyses of the static dimension (Fig. 3). This lack of consistency suggests that trade-offs and synergistic relationships between ES functions in the YRB differ depending on whether a static or dynamic dimension is considered. Using SL as a case study, in the static dimension, areas with high SL values are mainly located in landscapes such as sand dunes or deserts (Fig. 1), compared to the dynamic dimension, where SL is a more stable ES [42], showing a slightly increasing trend over the last 20 years (Fig. 2).

Driving Force Analysis of Ecosystem Services

This research investigates the factors influencing ecosystem services in the YRB over time through multiple linear regression analyses, utilizing various remote sensing datasets and terrestrial climate reanalysis data. Fourteen different variable indicators were chosen for assessment, including actual evapotranspiration (AET), soil moisture (SOIL), vegetation cover (NDVI), drought index (PDSI), solar radiation (SRAD), population density (POP), maximum temperature (TMMX), wind speed (VS), surface runoff (RO), imperviousness (IBI), potential evapotranspiration

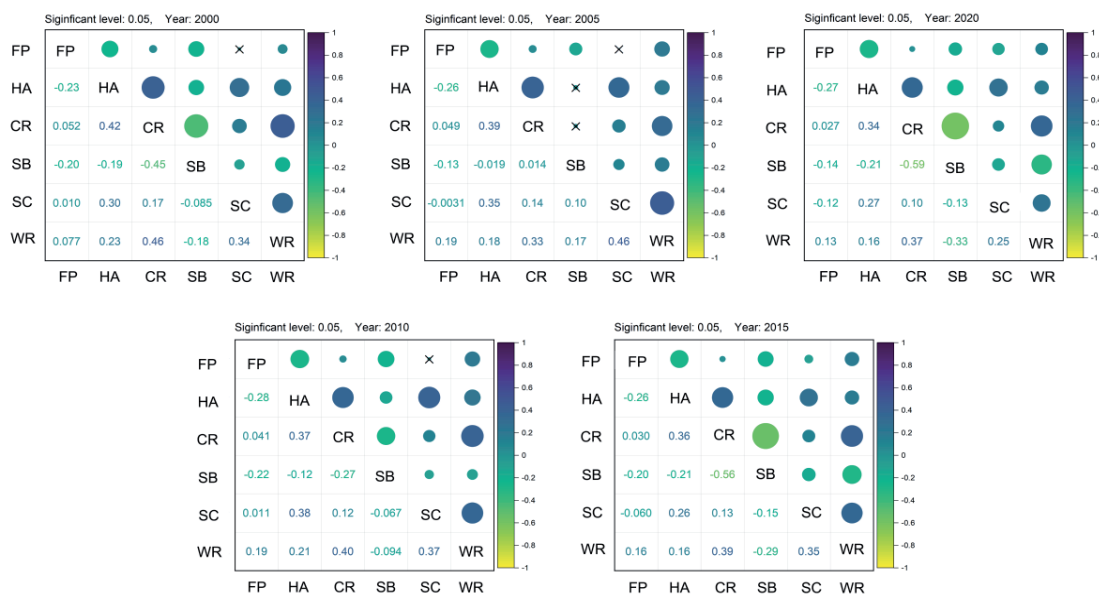


Fig. 3. Characteristics of ecosystem service trade-offs/synergies in the Yellow River Basin at the grid scale during 2000-2020.

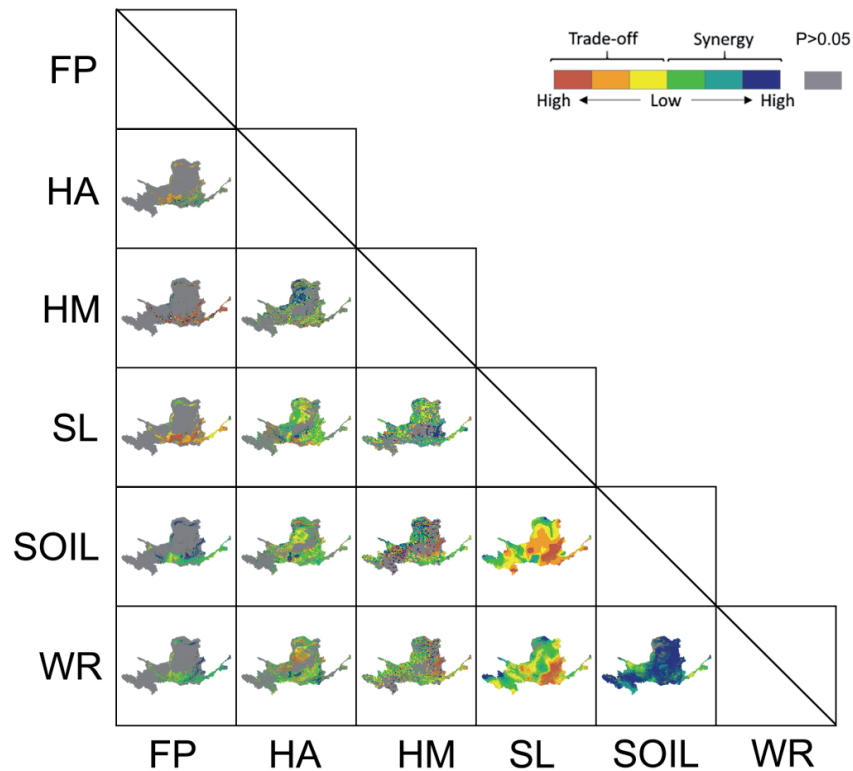


Fig. 4. Characteristics of ecosystem service trade-offs/synergies in the Yellow River Basin at the time scale during 2000-2020.

(PET), minimum temperature (TMMN), saturated water vapor pressure difference (VPD), and climatic water deficit (DEF). Fig. 5 shows the ranking (in descending order) of the degree of temporal driving of WR, HA, SR, FP, SL, and HM. Natural factors and human activities significantly impact the temporal changes of all ESs, with POP dominating in HA, FP, and SR and NDVI and AET dominating in WR and SL. Secondly, PET and RO had less influence on ecosystem services in the YRB. The analyses showed that the correlation effects of human activities and natural factors (climate change) had a wide range of influences on the YRB.

According to the results of this research, the following recommendations are suggested: Clarify the development objectives of the YRB and the conflicts of interest that may arise. To balance these conflicts, policies should be formulated based on ecosystem services. Land allocation for construction should be strictly controlled along rivers and in key ecological areas to ensure that key ecosystem services are not compromised. Meanwhile, the YRB should strengthen the synergy between conservation and development. Ecological mitigation and protection policies should be strictly enforced in areas with high ecosystem service values, such as important wetlands, estuaries, and biodiversity hotspots. When it comes to the utilization of land in urban and rural areas, scientific and rational land planning should be formulated to maximize land use efficiency, curb the disorderly expansion of urban areas, and vigorously promote the development of

new industries in harmony with ecological protection in order to reduce excessive consumption of natural resources. In addition, ecological land is being rationally allocated, key ecological corridors are being protected and restored, and a sustainable green design is being developed to promote a harmonious relationship between the natural environment and human actions.

Conclusions

Understanding the changes in the ecological environment of the YRB in light of the growing human activities and the impact of climate change on a global scale is essential to maintain the stability of the basin's biodiversity and the balance of the ecosystem. Therefore, this study used multi-source data to estimate the major environmental evaluations (food supply, habitat quality, soil conservation, water conservation, wind and sand control, and climate regulation) from 2000 to 2020.

By analyzing the spatial and temporal changes of ecosystem services in the YRB over the past two decades and exploring the trade-offs and synergistic effects between ecosystem services at the pixel scale, the study concludes the following: The ecosystem services in the YRB showed significant spatial heterogeneity during the study period but generally showed relative stability in the temporal dimension, and the ecosystem services of the YRB as a whole showed a middle and high value in the past 20 years. In the past 20 years, the ecosystem services in the YRB as a whole showed a

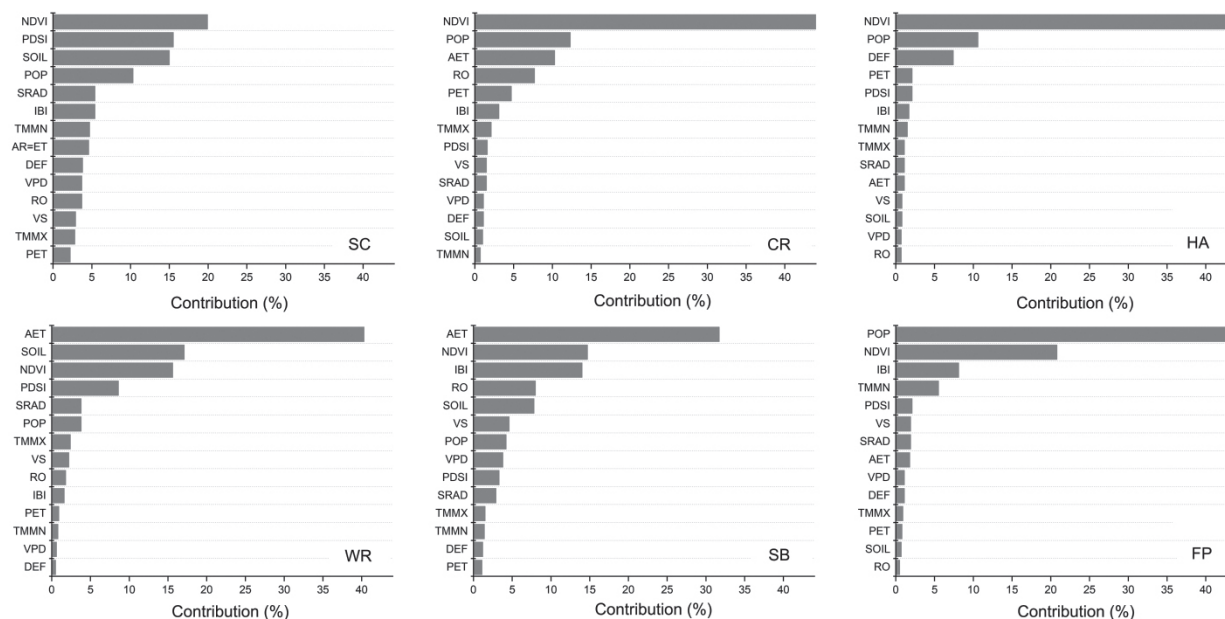


Fig. 5. Analysis of ecosystem service drivers in the Yellow River Basin during 2000-2020.

trend of gradual expansion of the middle and high-value zones and gradual reduction of the low-value zone. At the pixel scale (time dimension), most of the ecosystem services are in a weak synergistic relationship. Soil conservation (SOIL) showed synergistic relationships with other ecosystem services. Significantly, SL showed weak synergistic relationships with most ecosystem services (except FP) in the ever-changing realm of individual pixels. Finally, vegetation cover (NDVI) and human activities became the dominant factors driving the changes in ecosystem services in the YRB during the last 20 years.

In order to further promote the sustainable development of ecosystem services, it is recommended that the continuous monitoring of the spatiotemporal dynamics of ecosystem services, especially the in-depth analysis of the interaction between different ecosystem services at the pixel scale, be strengthened. Future research can focus on exploring how to achieve synergies in ecosystem services through scientific management and policy guidance, especially between soil conservation and other ecosystem services. In addition, vegetation cover and the impact of human activities will continue to be important research directions to improve ecosystem resilience and adaptability through developing adaptable management measures to meet changing environmental challenges.

In summary, this study aims to provide a scientific basis for the ecological protection and sustainable development of YRB, promote the in-depth implementation of ecological civilization construction, protect and restore the ecological environment, and provide more high-quality ecological products that meet human needs.

Acknowledgments

We would like to thank the Major Program of the National Social Science Foundation of China, "Innovation and Policy Research on Agricultural Green Development System under the 'Dual Carbon' Goals (22&ZD083)", for supporting this research.

Conflict of Interest

The authors declare that there is no conflict of interest.

References

1. BAI Y., OCHUODHO T.O., YANG J. Impact of land use and climate change on water-related ecosystem services in Kentucky, USA. *Ecological Indicators*. **102**, 51, **2019**.
2. ANDERSON S.J., ANKOR B.L., SUTTON P.C. Ecosystem service valuations of South Africa using a variety of land cover data sources and resolutions. *Ecosystem Services*. **27**, 173, **2017**.
3. CAPRIOLO A., BOSCHETTO R.G., MASCOLO R.A., BALBI S., VILLA F. Biophysical and economic assessment of four ecosystem services for natural capital accounting in Italy. *Ecosystem Services*. **46**, 101207, **2020**.
4. COSTANZA R., DE GROOT R., SUTTON P., VAN DER PLOEG S., ANDERSON S.J., KUBISZEWSKI I., FARBER S., TURNER R.K. Changes in the global value of ecosystem services. *Global Environmental Change-Human and Policy Dimensions*. **26**, 152, **2014**.
5. COSTANZA R., DE GROOT R., BRAAT L., KUBISZEWSKI I., FIORAMONTI L., SUTTON P., FARBER S., GRASSO M. Twenty years of ecosystem services: How far have we come and how far do we still need to go? *Ecosystem Services*. **28**, 1, **2017**.

6. GUO H., DONG S., WU D., PEI S., XIN X. Calculation and analysis of equivalence factor and yield factor of ecological footprint based on ecosystem services value. *Acta Ecologica Sinica*. **40** (4), 1405, **2020**.
7. ZHANG L., YU X., JIANG M., XUE Z., LU X., ZOU Y. A consistent ecosystem services valuation method based on Total Economic Value and Equivalent Value Factors: A case study in the Sanjiang Plain, Northeast China. *Ecological Complexity*. **29**, 40, **2017**.
8. YUAN L.G., GENG M.M., LI F., XIE Y.H., TIAN T., CHEN Q. Spatiotemporal characteristics and drivers of ecosystem service interactions in the Dongting Lake Basin. *Science of the Total Environment*. **926**, **2024**.
9. YUSHANJIANG A., ZHOU W., WANG J., WANG J. Impact of urbanization on regional ecosystem services – a case study in Guangdong-Hong Kong-Macao Greater Bay Area. *Ecological Indicators*. **159**, 111633, **2024**.
10. YAO X., ZHOU L., WU T., YANG X., REN M. Ecosystem services in National Park of Hainan Tropical Rainforest of China: Spatiotemporal dynamics and conservation implications. *Journal for Nature Conservation*. **80** (1), 126649, **2024**.
11. HUA Y., YAN D., LIU X. Assessing synergies and trade-offs between ecosystem services in highly urbanized area under different scenarios of future land use change. *Environmental and Sustainability Indicators*. **22** (3), 100350, **2024**.
12. XIONG K.N., KONG L.W., YU Y.H., ZHANG S.H., DENG X.H. The impact of multiple driving factors on forest ecosystem services in karst desertification control. *Frontiers in Forests and Global Change*. **6**, **2023**.
13. FANG G.J., SUN X., LIAO C., XIAO Y., YANG P., LIU Q.H. How do ecosystem services evolve across urban-rural transitional landscapes of Beijing-Tianjin-Hebei region in China: patterns, trade-offs, and drivers. *Landscape Ecology*. **38** (4), 1125, **2023**.
14. WANG S., SHI H., XU X., HUANG L., GU Q., LIU H. County zoning and optimization paths for trade-offs and synergies of ecosystem services in Northeast China. *Ecological Indicators*. **164**, 112044, **2024**.
15. DONG W., WU X., ZHANG J.J., ZHANG Y.L., DANG H., LÜ Y.H., WANG C., GUO J. Y. Spatiotemporal heterogeneity and driving factors of ecosystem service relationships and bundles in a typical agropastoral ecotone. *Ecological Indicators*. **156**, **2023**.
16. LIU L.H., ZHENG L., WANG Y., LIU C.C., ZHANG B.W., BI Y.Z. Land Use and Ecosystem Services Evolution in Danjiangkou Reservoir Area, China: Implications for Sustainable Management of National Projects. *Land*. **12** (4), **2023**.
17. XU Q., YANG Y., YANG R., ZHA L.S., LIN Z.Q., SHANG S.H. Spatial Trade-Offs and Synergies between Ecosystem Services in Guangdong Province, China. *Land*. **13** (1), **2024**.
18. WEN X., WANG J., HAN X. Impact of land use evolution on the value of ecosystem services in the returned farmland area of the Loess Plateau in northern Shaanxi. *Ecological Indicators*. **163**, 112119, **2024**.
19. DONG S., XU Y., LI S., SHEN H., YANG M., XIAO J. Restoration actions associated with payment for ecosystem services promote the economic returns of alpine grasslands in China. *Journal of Cleaner Production*. **458**, 142439, **2024**.
20. WANG S., ZHANG B., SHI Y.T., XIE G.D., WU Y.P., ZHU M.X. Exploring the combination and heterogeneity of ecosystem services bundles in the Beijing-Tianjin Sandstorm Source Control Project. *Ecological Indicators*. **155**, 110972, **2023**.
21. WANG X.Q., WANG B.J., CUI F.Q. Exploring ecosystem services interactions in the dryland: Socio-ecological drivers and thresholds for better ecosystem management. *Ecological Indicators*. **159**, 111699, **2024**.
22. SYRBE R.U., MEIER S., MOYZES M., DWORCZYK C., GRUNEWALD K. Assessment and Monitoring of Local Climate Regulation in Cities by Green Infrastructure-A National Ecosystem Service Indicator for Germany. *Land*. **13** (5), **2024**.
23. KLAUS V.H., SCHAUB S., SÉCHAUD R., FABIAN Y., JEANNERET P., LÜSCHER A., HUGUENIN-ELIE O. Upscaling of ecosystem service and biodiversity indicators from field to farm to inform agri-environmental decision- and policy-making. *Ecological Indicators*. **163**, 112104, **2024**.
24. PANDEY R., MEHTA D., KUMAR V., PRADHAN R.P. Quantifying soil erosion and soil organic carbon conservation services in indian forests: A RUSLE-SDR and GIS-based assessment. *Ecological Indicators*. **163**, 112086, **2024**.
25. SITOTAW T.M., WILLEMEN L., MESHESHA D.T., NELSON A. Empirical assessments of small-scale ecosystem service flows in rural mosaic landscapes in the Ethiopian highlands. *Ecosystem Services*. **67**, **2024**.
26. MIRCHOOI F., DABIRI Z., STROBL J., DARVISHAN A.K., SADEGHI S.H. Spatial and Temporal Dynamics of Rangeland Ecosystem Services Across the Shazand Watershed, Iran. *Rangeland Ecology & Management*. **90**, 45, **2023**.
27. XU J., XIAO Y., XIE G., WANG Y., ZHEN L., ZHANG C., JIANG Y. Interregional ecosystem services benefits transfer from wind erosion control measures in Inner Mongolia. *Environmental Development*. **34**, 100496, **2020**.
28. BHATTI U.A., YU Z., CHANUSSOT J., ZEESHAN Z., YUAN L., LUO W., NAWAZ S.A., BHATTI M., UI AIN Q., MEHMOOD A. Local Similarity-Based Spatial-Spectral Fusion Hyperspectral Image Classification With Deep CNN and Gabor Filtering. *IEEE Transactions on Geoscience and Remote Sensing*. **60**, 1, **2022**.
29. LI T., LI J., LIU J., HUANG M., CHEN Y-W., BHATTI U.A. Robust watermarking algorithm for medical images based on log-polar transform. *Journal on Wireless Communications and Networking*. **24**, **2022**.
30. BHATTI U.A., YUHUAN Y., MING-QUAN Z., ALI S., HUSSAIN A., QING-SONG H., YU Z., YUAN L. Time Series Analysis and Forecasting of Air Pollution Particulate Matter (PM_{2.5}): An SARIMA and Factor Analysis Approach. *IEEE Access*. **9**, 41019, **2021**.
31. BHATTI U.A., ZHOU M., HUO Q., ALI S., HUSSAIN A., YAN Y., YU Z., YUAN L., NAWAZ S.A. Advanced Color Edge Detection Using Clifford Algebra in Satellite Images. *IEEE Photonics Journal*. **13** (2), 1, **2021**.
32. BHATTI U.A., HUANG M., WANG H., ZHANG Y., MEHMOOD A., DI W. Recommendation system for immunization coverage and monitoring. *Human Vaccines & Immunotherapeutics*. **14** (1), 165, **2017**.
33. ZEESHAN Z., AIN Q., BHATTI U.A., MEMON W.H. Feature-based Multi-criteria Recommendation System Using a Weighted Approach with Ranking Correlation. *Intelligent Data Analysis*. **25** (4), 1013, **2021**.
34. BHATTI U.A., HUANG M., WU D., ZHANG Y., MEHMOOD A., HAN H. Recommendation system using feature extraction and pattern recognition in clinical care

- systems. *Enterprise Information Systems*. **13** (3), 329, **2018**.
35. ZENG C., LIU J., LI J., CHENG J., ZHOU J., NAWAZ S.A., XIAO X., BHATTI U.A. Multi-watermarking algorithm for medical image based on KAZE-DCT. *Journal of Ambient Intelligence and Humanized Computing*. **15** (9), 1, **2022**.
36. LIU W., LI J., SHAO C., MA J., HUANG M., BHATTI U.A. Robust Zero Watermarking Algorithm for Medical Images Using Local Binary Pattern and Discrete Cosine Transform. *ICAIS Communications in Computer and Information Science*. In Book: *Advances in Artificial Intelligence and Security*, Springer. **2022**.
37. LI Y., LI J., SHAO C., BHATTI U.A., MA J. Robust Multi-watermarking Algorithm for Medical Images Using Patchwork-DCT. *ICAIS Lecture Notes in Computer Science*. In book: *Artificial Intelligence and Security*, Springer. **2022**.
38. BHATTI U.A., NIZAMANI M.M., MENGXING H. Climate change threatens Pakistan's snow leopards. *Science*. **377** (6606), 585, **2022**.
39. BHATTI U.A., YUAN L., YU Z. New watermarking algorithm utilizing quaternion Fourier transform with advanced scrambling and secure encryption. *Multimedia Tools and Applications*. **80**, 13367, **2021**.
40. YI D., LI J., FANG Y., CUI W., XIAO X., BHATTI U.A., HAN B. A Robust Zero-Watermarking Algorithm Based on PHTs-DCT for Medical Images in the Encrypted Domain. In Book: *Innovation in Medicine and Healthcare Smart Innovation, Systems and Technologies*. Springer Singapore. **2021**.
41. XIAO X., LI J., YI D., FANG Y., CUI W., BHATTI U.A., HAN B. Robust Zero Watermarking Algorithm for Encrypted Medical Images Based on DWT-Gabor. In Book: *Innovation in Medicine and Healthcare Smart Innovation, Systems and Technologies*. Springer Singapore. **2021**.
42. FANG Y., LIU J., LI J., YI D., CUI W., XIAO X., HAN B., BHATTI U.A. A Novel Robust Watermarking Algorithm for Encrypted Medical Image Based on Bandelet-DCT. In Book: *Innovation in Medicine and Healthcare Smart Innovation, Systems and Technologies*. Springer Singapore. **2021**.